Rapid, Label-Free, Electrical Whole Blood Bioassay Based on Nanobiosensor Systems

Hsiao-Kang Chang,[†,⊥] Fumiaki N. Ishikawa,[†,⊥] Rui Zhang,[‡] Ram Datar,[§] Richard J. Cote,[§] Mark E. Thompson,[‡] and Chongwu Zhou[†,*]

[†]Departments of Electrical Engineering and [‡]Chemistry, University of Southern California, Los Angeles, California 90089, United States, and [§]Department of Pathology, University of Miami, Miami, Florida 33136, United States. [⊥]These authors contributed equally to the work.

ABSTRACT

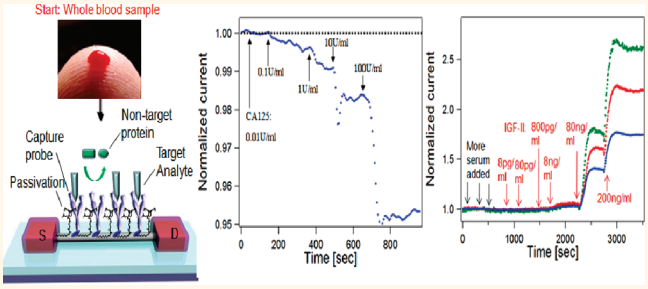

Biomarker detection based on nanowire biosensors has attracted a significant amount of research effort in recent years. However, only very limited research work has been directed toward biomarker detection directly from physiological fluids mainly because of challenges caused by the complexity of media. This limitation significantly reduces the practical impact generated by the aforementioned nanobiosensors. In this study, we demonstrate an In_2O_3 nanowire-based biosensing system that is capable of performing rapid, label-free, electrical detection of cancer biomarkers directly from human whole blood collected by a finger prick. Passivating the nanowire surface successfully blocked the signal induced by nonspecific binding when performing active measurement in whole blood. Passivated devices showed markedly smaller signals induced by nonspecific binding of proteins and other biomaterials in serum and higher sensitivity to target biomarkers than bare devices. The detection limit of passivated sensors for biomarkers in whole blood was similar to the detection limit for the same analyte in purified buffer solutions at the same ionic strength, suggesting minimal decrease in device performance in the complex media. We then demonstrated detection of multiple cancer biomarkers with high reliability at clinically meaningful concentrations from whole blood collected by a finger prick using this sensing system.

KEYWORDS: biosensor · nanowire · whole blood detection · cancer biomarker detection

Blood is one of the most informative sources for health and disease monitoring in the human body.[1,2] For example, monitoring levels of biomarkers in blood is known to be an effective method for early diagnosis of various diseases such as cancer, by which better treatment options and improved survival rates of patients can be provided.[3−7] Furthermore, therapeutic efficacy monitoring was demonstrated by following the levels of chosen biomarkers in blood before and after a therapy, which facilitates the physicians ability to determine the best treatment options.[8−11] Frequent monitoring of appropriate biomarkers is desirable for such purposes, since it leads to fast and timely feedback. This approach requires an easily accessible sensory platform that can monitor the level of biomarkers in a time-efficient and noninvasive (or negligibly invasive) manner with comparatively low cost and minimal pain for the patients. However, few existing systems satisfy all the aforementioned criteria. Thus, further research efforts are required toward realization of such a system.

Nanobiosensors have the potential to meet the aforementioned criteria because of the capability of performing rapid, label-free, electrical detection with potentially low cost. These devices utilize a capture agent on the sensor surface to bind the target biomolecules with both selectivity and specificity. The captured biomolecules affect the electronic properties of the nanowires, resulting in an electronically readable signal. Multiplexing has also been demonstrated by selectively functionalizing the nanowires with receptors for different biomarkers.[12] However, a challenge still remains toward making this technology more clinically practical. That is, the use of whole blood as an input is not typically investigated for biomarker detection, as such complex environments are known to cause problems such as false signal and saturation of receptors. The use of whole blood will allow evaluation of fragile proteins that experience prompt degradation after being taken out of the body as well as providing a simplified sample preparation protocol to expedite analysis.

* Address correspondence to chongwuz@usc.edu.

Received for review September 16, 2011 and accepted November 8, 2011.

Published online 10.1021/nn2035796

Recently significant progress has been made in biosensing from whole blood using a capture–release microfluidic chip[13] or from desalted serum;[12] however, more effort is needed for developing accurate and cost-effective systems that allow direct use of whole blood samples prepared using simple tools such as finger pricks. In addition, there is still a lack of understanding about biosensing using nanowires or nanotubes in complex media such as serum and plasma. In this report, we demonstrate a whole blood bioassay system based on nanowire sensors utilizing a custom-made microfilter and nanowire surface functionalization, which enabled rapid cancer biomarker detection directly from human whole blood collected by a finger prick, in a matter of minutes. The system developed here does not require any added reagents or sophisticated fabrication and is quite portable since it does not require any bulky equipment. The newly developed system consists of three parts: a sample processing system based on a custom-made microfilter, a sample delivery system based on a Teflon mixing cell, and a detection system based on the nanosensor array. By applying nanowire surface passivation, we observed suppression in signal induced by nonspecific serum proteins and enhancement in signal from the target analyte. We have applied the nanosensing system to perform cancer biomarker detection directly from human whole blood collected by a finger prick. Two cancer biomarkers associated with epithelial ovarian cancer, cancer antigen 125 (CA-125) and insulin-like growth factor II (IGF-II),[14–16] are successfully detected in real time. We achieved a 0.1 U/mL detection limit for CA-125 and an 8 ng/mL detection limit for IGF-II, which are at least 2 orders of magnitude lower than the clinically relevant level for diagnosis in both cases.[17–19] We also carried out in-depth analysis of sensing data from multiple devices to show that the nanosensor platform is highly reliable, giving consistent readings across several devices within an array and between arrays. The results indicate that such a system shows great potential to act as a future multiplexed diagnosis platform.

RESULTS AND DISCUSSION

The concept of our system for whole blood detection consists of three major functional components: (1) a sample processing system, (2) a sample delivery system, and (3) a detection system. The processing system is designed to process/purify human whole blood into a medium with which a sensor can retain its full sensitivity. The sample delivery system is to enable prompt delivery of the preprocessed samples to the detection system. The detection system consists of an array of nanobiosensors to achieve rapid, label-free, and electrical detection of the targets. In this study, we used a custom-designed microfilter to remove blood cells for the processing system and a mixing cell for the sample delivery system.

The operation of our system is as follows. About 500 μL of blood was collected by a commercially available finger prick device, allowed to clot, and passed through the microfilter to remove blood cells. The output of the microfilter (filtered whole blood) directly went to the mixing cell in order to achieve in-line detection. Schematic of the system setup is shown in Figure 1a. We used polycarbonate membranes with 400 nm pores for the filtration. The microscopic images of blood before and after filtration are shown in Figure 1b, and one can clearly see that the filtration removed almost all the blood cells. Insets of Figure 1b are the photo images of a blood sample before and after filtration. Shown in Figure 1c is the cell count in a blood sample before and after filtration, indicating the cell count was reduced by 99.6% after filtration. The result suggests that the microfilter can effectively remove blood cells and macroscopic impurities in whole blood, and the filtered whole blood is essentially serum.

We then delivered the filtered whole blood to the nanosensors for electrical measurement and assessed the sensor performance in the quasi-serum (filtrate of human whole blood through our filter) to investigate how the complexity of the medium impacts the sensor performance. All sensing experiments in this paper were conducted under an ionic strength of 1.5 mM. During the sensing experiment, a small source drain voltage (200 mV) is applied to the device, and the source drain current is measured and recorded in real time using an Agilent B1500 semiconductor analyzer. The measured device current can be normalized or calibrated to reduce device-to-device variation when comparing data from different devices. Details of this analysis are described in our previous publication.[20]

To illustrate the problems caused by nonspecific binding of the nontarget proteins in serum, we compare the performances of nanosensors in buffer and quasi-serum of the same ionic concentration side-by-side using CA-125, an epithelial ovarian cancer biomarker, as model. Both nanosensors used here are prepared in an identical manner, with the In_2O_3 nanowires coated with the CA-125 antibody. Details of device fabrication and functionalization are described in the Methods section and are similar to previously published procedures.[21–25] In_2O_3 nanowires have been previously studied for chemical sensing, biosensing, memory, and transistor applications.[26–29] We note that the metal electrodes are conformally coated with a silicon nitride layer (SEM image shown in Supporting Information) to ensure the signal observed is from nanowires rather than metal electrodes. Device characteristics of three devices are shown in the Supporting Information, displaying strong gate dependence and good uniformity of device performance within the

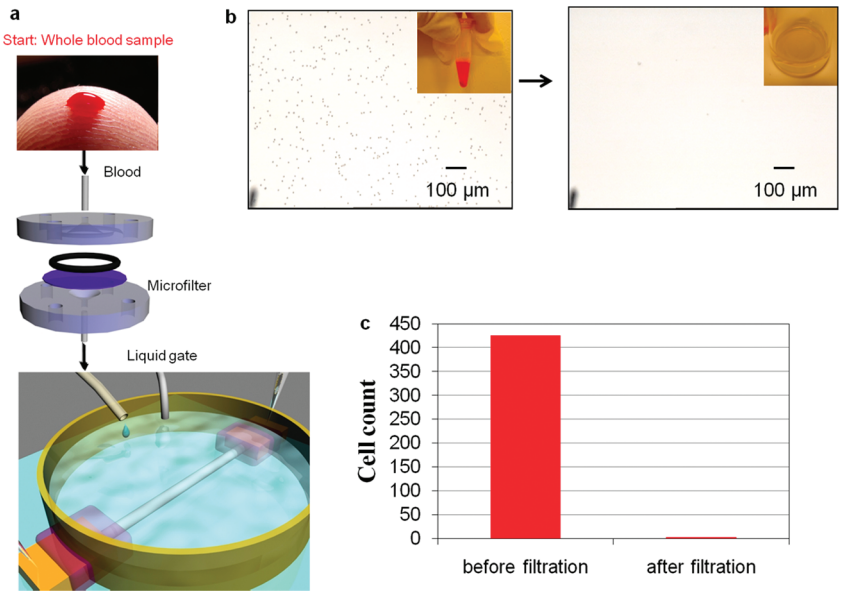

Figure 1. (a) Schematic of system configuration. (b) Microscopic and photo (inset) image of blood sample before and after microfiltration. (c) Cell count before and after microfiltration.

array. As a control experiment, an In_2O_3 nanowire biosensor was first submerged in 1.5 mM phosphate buffered saline (PBS) using the mixing cell, and then a drop of CA-125 solution in 1.5 mM PBS was added to achieve a final concentration of 1 U/mL (5 pM) CA-125. Figure 2a shows the device configuration and real-time sensing response for the above-mentioned device. The source–drain current decreased and re-equilibrated to a lower level after being introduced to 1 U/mL CA-125 with the change in current about 1%. As a comparison, shown in Figure 2b is the real-time sensing response for a device submerged in serum and then exposed to CA-125 of 1 U/mL concentration, and there is no noticeable sensing signal. These two aforementioned experiments were preformed with identical devices, under similar ionic concentration (hence comparable Debye length). Nontarget proteins in serum are known to negatively impact the sensitivity of nanosensors. We attributed the loss of sensing response in serum to blocking of binding sites of the target by nonspecific binding. Further in-depth study suggests that the complexity of a medium substantially limits the sensing performance of nanosensors due to nonspecific binding, as shown in Supporting Information Figure S3. There is clearly a need for development of a strategy to enhance the sensing performance in complex media for these devices.

In order to overcome the limitation induced by nonspecific binding of nontarget proteins, we used an amphipathic polymer, Tween 20, as the passivating agent on the nanowire surface to reduce nonspecific binding. Tween 20 is often used as a blocking agent in bioanalytical assays. The polymer minimizes nonspecific binding[30] due to its low binding affinity to the abundant proteins present in physiological fluids. Shown in Figure 2c is the device schematics after Tween 20 functionalization. To prepare devices with Tween 20 functionalization, we submerged fabricated nanowire biosensors in 50 μg/mL Tween 20 in PBS for 1 h after the antibody immobilization step. This Tween 20 functionalization does not adversely affect the device performance of the biosensor, as the gate dependence of the device, using a liquid gate, is the same before and after Tween 20 passivation (see Supporting Information). The normalized current *versus* time plot for a device with Tween 20 passivation is also displayed in Figure 2c, demonstrating the sensitive detection of CA-125 in the quasi-serum environment. The passivated device is able to successfully detect 1 U/mL CA-125 in serum with a sensing signal magnitude (1% reduction in current) similar to the device in purified buffer (Figure 2a). Our results clearly suggest that by applying Tween 20 passivation to the nanowire surface, we can retain excellent sensing performance, even in a complex medium such as serum.

To further study the effect of Tween 20 passivation on the sensor performance, we compared the signals caused by nonspecific binding from four types of devices with distinct surfaces using the well-studied biotin–streptavidin conjugation as a model. These four types include bare In_2O_3 nanowire devices, biotin-conjugated In_2O_3 nanowire devices without further passivation, bare In_2O_3 nanowire devices passivated by Tween 20, and biotin-conjugated In_2O_3 nanowire devices passivated by Tween 20. We measured the change in the nanowire biosensor current (ΔI) upon exposure to serum for all four types of devices, and the calibrated responses (as calculated using $\Delta I/g_m$ following ref 20) induced by nonspecific binding are

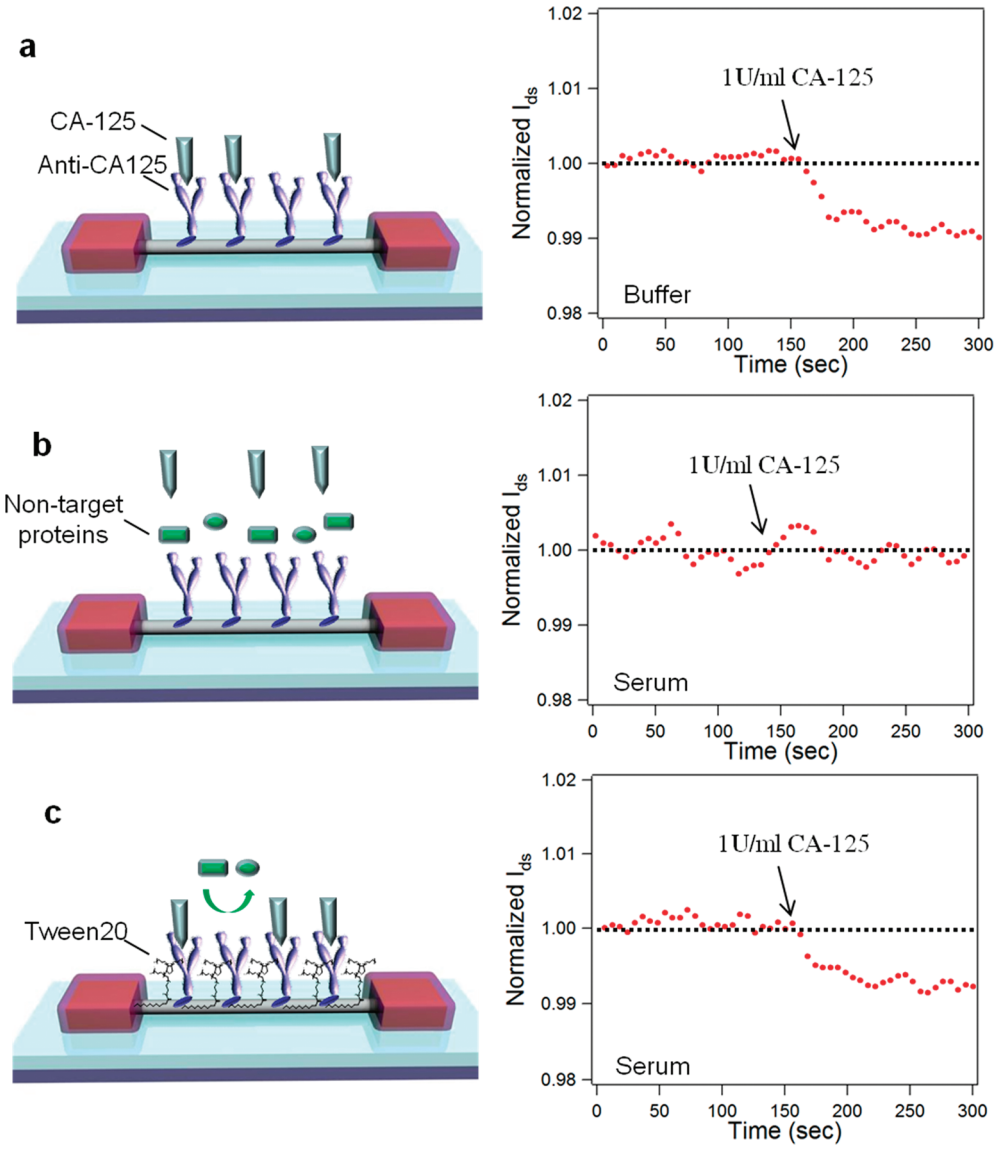

Figure 2. Device configuration and real-time sensing response for (a) unpassivated CA-125 nanosensor in buffer, (b) unpassivated CA-125 nanosensor in serum, and (c) Tween 20-passivated nanosensor in serum (inset: structure of Tween 20).

shown in Figure 3a. The responses are 62.2 mV for bare devices, 36.4 mV for biotin-conjugated devices, 3.3 mV for bare devices passivated by Tween 20, and 5.1 mV for biotin-conjugated devices passivated by Tween 20. The results clearly show that Tween 20 coating can significantly suppress the amount of nonspecific binding, which has been considered to be a major issue for nanowire-based biosensors.

In addition, we carried out further experiments to show that incorporation of surface functionalization would not degrade the sensing performance (limit of detection and magnitude of responses) of nanosensors in complex media, as shown below, where we compared the calibrated response of devices in various media and with/without Tween 20 passivation. Two media including phosphate-buffered saline and serum were used. All the devices were functionalized with biotin, and then selected devices were further passivated with Tween 20. All the devices were exposed to streptavidin of 1, 10, and 100 nM concentrations in each medium under constant ionic strength of 1.5 mM. The result is shown in Figure 3b. For unpassivated devices in PBS, the calibrated responses (green curve) to streptavidin of 1, 10, and 100 nM are 1.37, 6.2, and 15.8 mV, respectively. The device showed no observable response to 100 pM streptavidin. For bare devices in serum, the sensing response (blue curve) was significantly lower than those in pure buffer (green curve), and the detection limit was 10 nM, which was 1 order of magnitude worse than the detection limit in buffer. We repeated the aforementioned sensing experiment in serum with Tween 20-passivated devices. The detection limit of those devices was 1 nM, which is the same as the detection limit in buffer. The calibrated responses (red curve) are significantly higher than the response from nonpassivated devices as well, and

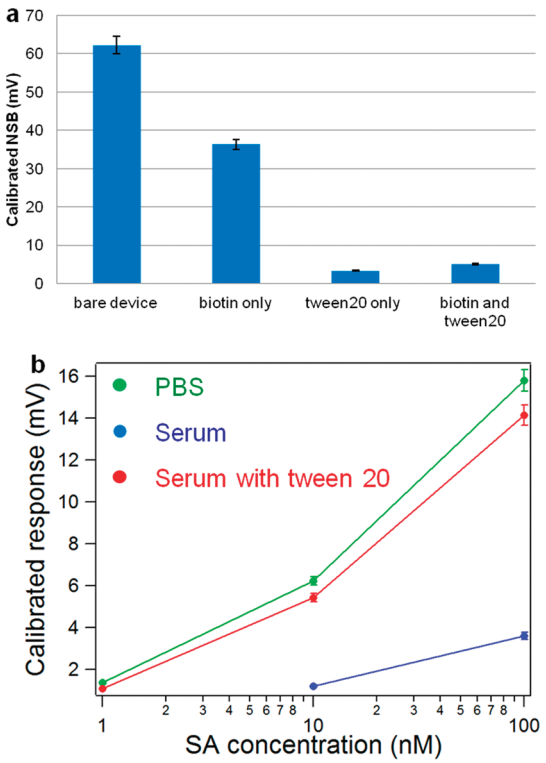

Figure 3. In-depth study of nanowire surface passivation. (a) Calibrated nonspecific binding induced by blood proteins for devices of different surface functionalizations. (b) Calibrated response *versus* streptavidin concentration for both passivated and unpassivated devices in various media.

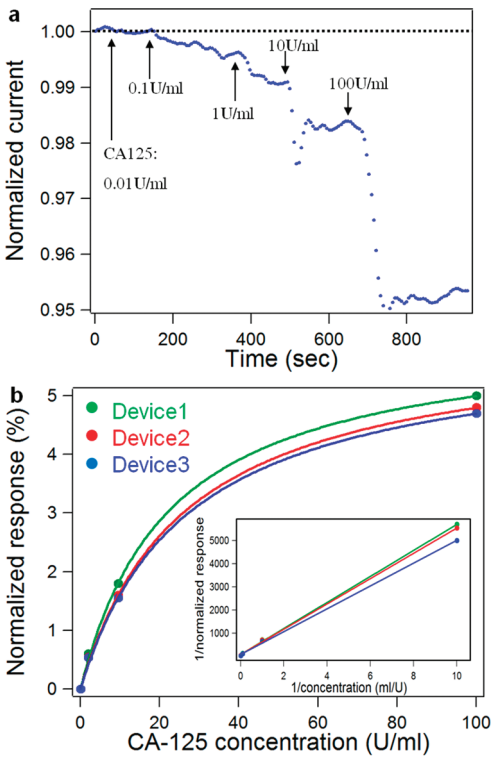

Figure 4. CA-125 detection in whole blood. (a) Normalized device current *versus* time during active CA-125 measurement in whole blood. (b) Normalized response from three CA-125 biosensors *versus* concentration of CA-125 (dots). These plots can be fitted with a Langmuir isotherm model. (solid line) Inset: 1/response *vs* 1/concentration showing a linear fit.

reached 1.1, 5.4, and 14.2 mV to 1, 10, and 100 nM streptavidin, respectively. Those sensing responses for the Tween 20-passivated device in serum are almost as high as what we observed in buffer, and the detection limit is the same. The experimental data suggest that by suppressing the nonspecific binding, the Tween 20-passivated biosensors can be as sensitive in serum as bare biosensors in buffer, which is crucial for biosensing applications.

Now that the important role of Tween 20 surface functionalization has been fully elucidated, we moved on to concentration-dependent detection of cancer antigen 125 (CA-125) and insulin growth factor II (IGF-II), two biomarkers associated with epithelial ovarian cancer, in filtered whole blood as a demonstration toward a multiplexed whole blood cancer diagnosis system using nanobiosensors. An array of In_2O_3 nanowire sensors were first functionalized with anti-CA125 antibody through a previously developed procedure.[31] After antibody immobilization, the device was submerged in 50 μg/mL Tween 20 for 1 h. During the sensing experiment, the device was first washed in 1.5 mM PBS. Control serum was collected from a healthy cancer-free person using the above-mentioned finger-pricking and filtration technique and then diluted by a factor of 100 to achieve the same ionic strength of 1.5 mM. The diluted control serum was then added to the mixing cell to prepare the biosensor for detection. Shown in Figure 4a is the plot of the normalized current *versus* time while the device was exposed to an increased concentration of CA-125 consecutively. CA-125 was added to give the sample final concentrations of 0.01, 0.1, 1 (5 pM), 10, and 100 U/mL in the medium. The device showed no response to 0.01 U/mL CA-125, but showed a decrease in conductance when exposed to 0.1 U/mL CA-125. The responses became more significant when the device was exposed to CA-125 of higher concentrations. We note that CA-125 was detected under the presence of serum proteins of much higher concentration, therefore confirming the specificity of the nanobiosensors. Here the Debye screening effect was reduced by diluting the serum sample, which reduced the ionic strength to 1.5 mM (as compared to 150 mM before dilution) and enabled good performance for CA-125 sensing. The detection limit of 0.1 U/mL CA-125 would correspond to a concentration of 10 U/mL in the original serum before dilution, which is much lower than the clinically relevant level for the diagnosis of ovarian cancers (100−275 U/mL),[16] therefore confirming the practical value of our sensors.

Three devices were tested in parallel during the CA-125 sensing experiment, and all the devices showed quantitatively similar concentration dependence for

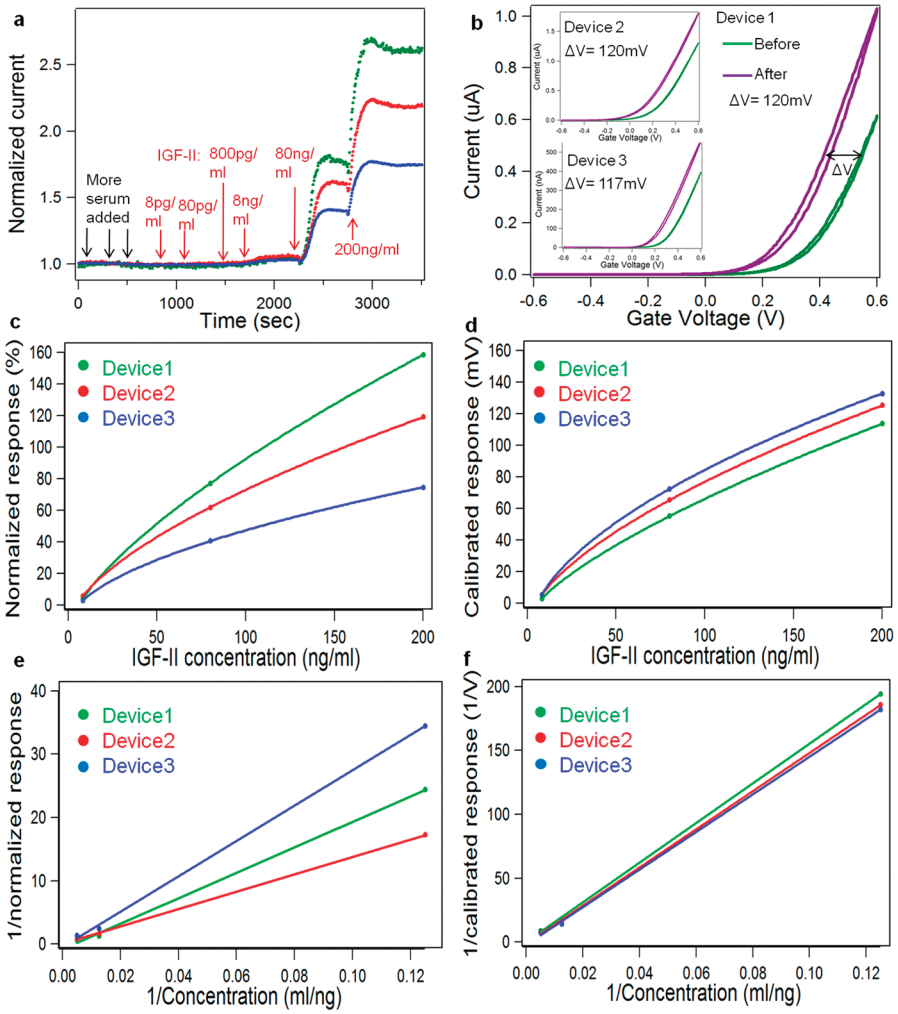

Figure 5. IGF-II detection with integratable gravity desalting column. (a) Real-time IGF-II sensing response with three nanosensors. (b) Current-gate voltage characteristics for the three devices before (green curves) and after (purple curves) IGF-II binding. ΔV stands for the shift of $I-V$ curve induced by electrostatic interaction of IGF-II. (c) Normalized response ($\Delta I/I_0$) *versus* concentration for the three devices tested. (d) Calibrated response ($\Delta I/g_m$) *versus* concentration for the three devices tested. (e) Inverse of normalized response *versus* inverse of concentration for the three devices tested (dots) and their linear fits (solid lines). (f) Inverse of normalized response *versus* inverse of concentration for the three devices tested (dots) and their linear fits (lines).

their responses. Plots of sensor response *versus* CA-125 concentration for all three devices are shown in Figure 4b (dots), confirming the reproducibility of the results. These plots were fitted using the Langmuir isotherm model[32,33] (solid line), and these fits were used to estimate the dissociation constant of CA-125 antibody and antigen. When applying this model, we assumed that the response of the sensor is proportional to the number of captured molecules on the sensor surface, such that $\Delta I/I_0 \propto$ CA-125 surface coverage. The following equation was used to describe the concentration dependence of our sensor response following the Langmuir isotherm model:

$$\Delta I/I_0 = A\frac{\alpha n}{1+\alpha n}$$

where A is a coefficient that relates surface coverage ($\alpha n/(1+\alpha n)$) to electrical response ($\Delta I/I_0$), α is the Langmuir adsorption constant, and n is the concentration of CA-125. The values of A and α were determined using the least-squares method to give the best fit to the experimental values. The equation above can be rewritten to predict a linear relation between $I_0/\Delta I$ and $1/n$. Figure 4b inset shows plots of $I_0/\Delta I$ (1/normalized response) *versus* $1/n$ (1/concentration), and the data points from all three devices can be very well fitted with linear curves, thus confirming the Langmuir isotherm model. The dissociation constant was estimated by calculating the solution of n in the following equation:

$$\theta = \Delta I/I_0\frac{1}{A} = \frac{\alpha n}{1+\alpha n} = 0.5$$

where θ is the percentage coverage of the surface, since the definition of dissociation constant is an analyte concentration where half of the binding sites are occupied by the antigen. Application of this

analytical model yields a dissociation constant of 35.7 ± 2.8 U/mL (178.5 ± 14 pM), and a similar fitting has been applied to nanobiosensors in our previous publication.[34]

The second epithelial ovarian cancer biomarker we target in this work is IGF-II. The antibody functionalization technique is similar to CA-125 nanosenors. Here the ionic strength was reduced by using a gravity desalting column (purchased from Thermo Scientific). As a result, the Debye screening effect was reduced, which allowed us to achieve good sensitivity without diluting the sample. We note that the gravity desalting column is very compact and can be fully integrated into the sample processing system without any bulky equipment such as a centrifuge. This is different from the desalting column in ref 12, which requires a centrifuge and hence human intervention. The nanosensors were first immersed in 1.5 mM PBS, and then desalted human serum was added to replace the buffer. IGF-II antigen was then progressively added to the mixing cell to achieve final concentrations of 8 pg/mL, 80 pg/mL, 800 pg/mL, 8 ng/mL, 80 ng/mL, and 200 ng/mL. The normalized current *versus* time for three devices is monitored simultaneously with results plotted in Figure 5a. Once the devices were stabilized in desalted serum, they showed no response to further addition of serum (and hence increased serum protein concentration). In contrast, all three devices showed a positive sensing response to IGF-II at concentrations of 8 ng/mL and beyond. This limit of detection is 2 orders of magnitude lower than the clinically relevant level for diagnosis.[16] The three devices showed a very similar trend of response with some difference in magnitude. This difference resulted from device-to-device variation in transconductance of nanosenors and can be calibrated by considering the gating effect induced by the target analyte, as reported in our previous publication.[20] In order to further study the reproducibility of the electrostatic gating effect caused by the target analyte, we characterize the gate dependence using a liquid gate for all three devices before and after the addition of IGF-II. We then consider the magnitude of the electrostatic gating effect (ΔV) induced by IGF-II for all devices tested, and the results are shown in Figure 5b and insets. The ΔV for device 1, 2, and 3 are 120, 120, and 117 mV, respectively. This result indicates that our devices exhibit uniform electrostatic interaction to target analytes and are able to serve as highly reliable sensors. Figure 5c and d show a normalized response ($\Delta I/I_0$) and calibrated response ($\Delta I/g_m$) *versus* concentration for the three devices tested, respectively, with dots for experimental and fitted curves using the Langmuir isotherm model. The small dispersion in curves in Figure 5d confirmed calibration is more effective in minimizing device-to-device variation than normalization, as reported in our previous publication.[20] Figure 5e and f show the inverse of normalized and the inverse of calibrated response *versus* the inverse of IGF-II concentration, respectively. The experimental data (dots) can be fitted well linearly (solid lines) and, thus, confirmed the conjugation between IGF-II antibody and antigen fits the Langmuir isotherm model. Note that with the detection of multiple EOC biomarkers (CA-125 and IGF-II), demonstrated with a limit of detection much lower than the clinically relevant level for diagnosis in each case, our nanosensor system shows great potential to act as a stepping stone toward a multiplexed diagnosing tool for diseases such as cancer.

CONCLUSION

In conclusion, we have demonstrated a nanowire-based biosensing system that is able to achieve rapid, label-free, electrical biomolecule detection directly from whole blood collected by a finger prick. Nanowire surfaces were passivated with Tween 20 to suppress nonspecific binding induced by proteins in physiological fluid and thus enhance sensing performance in complex media. An experiment was conducted to demonstrate that Tween 20-passivated nanosensors show an improved limit of detection and more significant response to the target analyte than that of non-passivated devices. The nonspecific binding in serum is also noticeably smaller. We then demonstrated detection of two epithelial ovarian cancer biomarkers, CA-125 and IGF-II, in whole blood with detection limits significantly lower than the clinically relevant levels for diagnosis. A study of electrostatic gating effect induced by a target analyte further confirms the reliability of the nanosensors. We also emphasize that the whole operation of ovarian cancer biomarker detection was done in a simple, rapid, and cost-efficient manner from blood collection by a finger prick, filtration through the microfilter without any bulky equipment, to the detection with nanobiosensors. The system thus has a high potential toward a fully portable diagnosis system that is ideal for point-of-care type treatments. This study represents a significant step forward toward the clinical application of nanobiosensors such as disease diagnosis and drug efficacy monitoring.

METHODS

Materials. Phosphate buffer saline (pH 7.40, 10 mM phosphates, 137 mM NaCl, 2 mM KCl) was purchased from Mediatech Inc. CA-125 antigen and antibody were purchased from Fitzgerald. Tween-20, biotin-PEG-amine, IGF-II antibody, and antigen were purchased from Sigma-Aldrich. Streptavidin was purchased from Invitrogen. *N*-Hydroxysuccinimide (NHS) was purchased from Thermo Scientific.

Device Fabrication. In_2O_3 nanowires were grown *via* a laser ablation CVD method. Details of the nanowire growth are described in literature previously published by us.[21−25] The nanowires so grown were suspended in isopropyl alcohol by ultrasonication, and this suspension was deposited onto another whole Si/SiO_2 wafer with a density of about 1 nanowire per 100 μm^2. The source and drain (S−D) electrodes were defined by photolithography. The S−D electrodes were designed to have an interdigitated interface at the semiconductor channel, leading to FETs with channel length and width of 2.5 and 780 μm, respectively. Metal (5 nm of Cr, 50 nm of Au, and 3 nm of Ni) and silicon nitride (about 40 nm) were then deposited on the prepatterned surface. The nitride was conformally coated on the metal by Plasmatherm 790 PECVD to prevent signal induced by proteins bound to metal electrodes nonspecifically. Finally, a lift-off process and selective dry etch to expose electrodes were performed to complete the device fabrication.

Surface Functionalization. In_2O_3NW devices fabricated by the aforementioned method went through a standard cleaning process before any surface functionalization. The devices were then dried and placed in an ozone/UV chamber for 2 min. Immediately after cleaning, the nanowire devices were submerged in a 0.1 mM aqueous solution of 3-phosphonopropionic acid for 16 h at room temperature, resulting in the binding of the phosphonic acid residue to the surface of the In_2O_3 NWs. These devices were baked at 120 °C under nitrogen for 12 h. These devices were then wired on a custom-made printed circuit board, and a mixing cell was assembled on the device chip. This mixing cell was used to deliver and handle all the chemical reagents necessary for surface modification and the human whole blood during active measurements. The carboxylic acid functional groups on the NW surface were activated by a NHS/EDC aqueous solution for 45 min. This resulted in a NW surface reactive toward the amine groups present on antibodies. The NHS/EDC solution was removed from the mixing cell by progressive dilution with DI water. A solution containing antibody was allowed to react with the NW surface overnight at 4 °C. This antibody solution was replaced with 1× PBS by progressive dilutions. Finally the devices were treated with 50 μg/mL Tween 20 for 1 h before the sensing experiment.

Integratable Gravity Desalting Column. The gravity desalting column was purchased from Thermo Scientific. The column was first equilibrated with buffer following the protocol. The serum was then passed through the column. The absorption spectrum of elution was measured to confirm the majority of proteins are retained. The elution was ready to be delivered to the nanosensors for the sensing experiment.

Acknowledgment. The authors acknowledge financial support from the L.K. Whittier Foundation, the National Institutes of Health, and the National Science Foundation (CCF-0726815, 5RO1EB8275, and CCF-0702204).

Supporting Information Available: Cross-sectional SEM image of metal electrode coated with nitride (S1). Nanosensor device characteristics (S2). Streptavidin detection with nanosensors with and without passivation (S3). Characteristics of a device after Tween 20 passivation (S4). Nonspecific binding in serum for bare devices (S5). Nonspecific binding in serum for passivated devices (S6). Streptavidin detection in buffer (S7). OPN detection in whole blood (S8). Images of nanosensor system (S9). This material is available free of charge *via* the Internet at http://pubs.acs.org.

REFERENCES AND NOTES

1. Fujii, K.; Nakano, T.; Kanazawa, M.; Akimoto, S.; Hirano, T.; Kato, H.; Nishimura, T. Clinical-scale High-throughput Human Plasma Proteome Clinical Analysis: Lung adenocarcinoma. *Proteomics* **2005**, *5*, 1150–1159.
2. Lathrop, J. T.; Anderson, N. L.; Anderson, N. G.; Hammond, D. J. Therapeutic Potential of the Plasma Proteome. *Curr. Opin. Mol. Ther.* **2003**, *5*, 250–257.
3. Carlsson, A.; Wingren, C.; Ingvarsson, J.; Ellmark, P. Baldertorp, B.; Ferno, M.; Olsson, H.; Borrebaeck, C. A. K. Serum Proteome Profiling of Metastatic Breast Cancer Using Recombinant Antibody Microarrays. *Eur. J. Cancer* **2008**, *44*, 472–480.
4. Lee, M.; Im, J.; Lee, B. Y.; Myung, S.; Kang, J.; Huang, L.; Kwon, Y. K.; Hong, S. Linker-free Directed Assembly of High-performance Integrated Devices Based on Nanotubes and Nanowires. *Nat. Nanotechnol.* **2006**, *1*, 66–71.
5. Borgia, J. A.; Basu, S.; Faber, L. P.; Kim, A. W.; Coon, J. S.; Kaiser-Walters, K. A.; Fhied, C.; Thomas, S.; *et al*. Establishment of a Multi-Analyte Serum Biomarker Panel to Identify Lymph Node Metastases in Non-small Cell Lung Cancer. *J. Thorac. Oncol.* **2009**, *4*, 338–347.
6. Greenwood, P. B.; Hiraoka, M.; Evans, M. A Novel, 4 Biomarker Panel (Birthstat) for the Serum Detection of Parturition in the Term and Pre-term Period. *Am. J. Obstet. Gynecol.* **2006**, *195*, S44–S44.
7. Kuzdzal, S. A.; Lopez, M. F.; Mikulskis, A.; Sarracino, D.; O'Gorman, M.; Patton, W.; Rosenblatt, K.; Gurnani, P.; *et al*. Identification of a Four Marker Biomarker Panel from the Serum Fragmentome for Classification of Stage 1 Ovarian Cancer. *Mol. Cell. Proteomics* **2006**, *5*, S18–S18.
8. Oikonomopoulou, K.; Li, L.; Zheng, Y.; Simon, I.; Wolfert, R. L.; Valik, D.; Nekulova, M.; Simickova, M.; Frgala, T.; Diamandis, E. P. Prediction of Ovarian Cancer Prognosis and Response to Chemotherapy by a Serum-based Multiparametric Biomarker Panel. *Br. J. Cancer* **2008**, *99*, 1103–1113.
9. Mitani, Y.; Oue, N.; Matsumura, S.; Yoshida, K.; Noguchi, T.; Ito, M.; Tanaka, S.; Kuniyasu, H.; Kamata, N.; Yasui, W. Reg IV is a Serum Biomarker for Gastric Cancer Patients and Predicts Response to 5-Fluorouracil-based Chemotherapy. *Oncogene* **2007**, *26*, 4383–4393.
10. Nolen, B. M.; Marks, J. R.; Ta'san, S.; Rand, A.; Luong, T. M.; Wang, Y.; Blackwell, K.; Lokshin, A. E. Serum Biomarker Profiles and Response to Neoadjuvant Chemotherapy for Locally Advanced Breast Cancer. *Breast Cancer Res.* **2008**, 10.
11. Olofsson, M. H.; Ueno, T.; Pan, Y.; Xu, R.; Cai, F.; van der Kuip, H.; Muerdter, T. E.; Sonnenberg, M.; *et al*. Cytokeratin-18 is a Useful Serum Biomarker for Early Determination of Response of Breast Carcinomas to Chemotherapy. *Clin. Cancer Res.* **2007**, *13*, 3198–3206.
12. Zheng, G. P., F.; Cui, Y.; Wang, W. U.; Lieber, C. M. Multiplexed Electrical Detection of Cancer Markers with Nanowire Sensor Arrays. *Nat. Biotechnol.* **2005**, *23*, 1294–1301.
13. Stern, E. V., A.; Rajan, N. K.; Criscione, J. M.; Park, J.; Ilic, B. R.; Mooney, D. J.; Reed, M. A.; Fahmy, T. M. Label-free Biomarker Detection from Whole Blood. *Nat. Nanotechnol.* **2010**, *5*, 138–142.
14. Mor, G. V. I.; Feng, Z. D.; Longton, G.; Ward, D. C.; Alvero, A. B. Diagnostic Markers for Early Detection of Ovarian Cancer. *Cancer Biomarkers* **2008**, *4*, 190–191.
15. Steffiensen, K. D. W. M.; Visintin, I.; Brandslund, I.; Jakobsen, A.; Mor, G. Multiplex Serum Tumor Markers for the Prediction of Early Relapse in Ovarian Cancer Patients. *Reprod. Sci.* **2008**, *15*, 856.
16. Visintin, I. F. Z.; Longton, G.; Ward, D. C.; Alvero, A. B.; Lai, Y. L. Diagnostic Markers for Early Detection of Ovarian Cancer. *Clin. Cancer Res.* **2008**, *14*, 1065–1072.
17. Juretzka, M. M, B. R.; Chi, D. S.; Iasonos, A.; Dupont, J.; Abu-Rustum, N. R.; Poynor, E. A.; Aghajanian, C.; Spriggs, D.; Hensley, M. L.; *et al*. CA125 Level as a Predictor of Progression-free Survival and Overall Survival in Ovarian Cancer Patients with Surgically Defined Disease Status Prior to the Initiation of Intraperitoneal Consolidation Therapy. *Gynecol. Oncol.* **2007**, *104*, 176–180.
18. Tian, CQ, M. M.; Zaino, R; Ozols, R. F.; McGuire, W. P.; Muggia, F. M.; Rose, P. G.; Spriggs, D; Armstrong, D. K. CA-125 Change After Chemotherapy in Prediction of Treatment Outcome Among Advanced Mucinous and Clear Cell Epithelial Ovarian Cancers A Gynecologic Oncology Group Study. *Cancer* **2009**, *115*, 1395–1403.
19. Balbi, GC, C. A.; Passaro, M; Battista, M; Monteverde, A; Visconti, S. Comparative Evaluation of Standard Criteria

and CA-125 in Ovarian Cancers Treated with Platinum or Paclitaxel. *Eur. J. Gynaecol. Oncol.* **2005**, *26*, 285–287.
20. Ishikawa, F. N. C., M.; Chang, H. K.; Chen, P. C.; Zhang, R.; Cote, R. J.; Thompson, M. E.; Zhou, C. A Calibration Method for Nanowire Biosensors to Suppress Device-to-Device Variation. *ACS Nano* **2009**, *3*, 3969–3976.
21. Li, C. C., M.; Lin, H.; Lei, B.; Ishikawa, F. N.; Datar, R.; Cote, R. J.; Thompson, M. E.; Zhou, C. W. Complementary Detection of Prostate-Specific Antigen Using In_2O_3 Nanowires and Carbon Nanotubes. *J. Am. Chem. Soc.* **2005**, *127*, 12484–12485.
22. Liu, F. B., M.; Wang, K. L.; Li, C.; Lei, B.; Zhou, C. One-Dimensional Transport of In_2O_3 Nanowires. *Appl. Phys. Lett.* **2005**, *86*, 213101–213103.
23. Curreli, M. L., C.; Sun, Y. H.; Lei, B.; Gundersen, M. A.; Thompson, M. E.; Zhou, C. W. Selective Functionalization of In_2O_3 Nanowire Mat Devices for Biosensing Applications. *J. Am. Chem. Soc.* **2005**, *127*, 6922–6923.
24. Lei, B. L., C.; Zhang, D.; Tang, T.; Zhou, C. Tuning Electronic Properties of In_2O_3 Nanowires by Doping Control. *Appl. Phys. A: Mater. Sci. Process.* **2004**, *79*, 439–442.
25. Li, C. Z., D.; Han, S.; Liu, X.; Tang, T.; Lei, B.; Liu, Z.; Zhou, C. Synthesis, Electronic Properties, and Applications of Indium Oxide Nanowires. *Ann. N. Y. Acad. Sci.* **2003**, *1006*, 104–121.
26. Li, C.; Ly, J.; Lei, B.; Fan, W.; Zhang, D.; Han, J.; Meyyappan, M.; Thompson, M.; Zhou, C. Data Storage Studies on Nanowire Transistors with Self-assembled Porphyrin Molecules. *J. Phys. Chem. B* **2004**, *108*, 9646–9649.
27. Li, C.; Lei, B.; Zhang, D. H.; Liu, X.; Song, H.; Tao, T.; Mahsa, R.; Tzung, H.; Zhou, C. Chemical Gating of In_2O_3 Nanowires by Organic and Biomolecules. *Appl. Phys. Lett.* **2003**, *83*, 4014–4016.
28. Lei, B.; Li, C.; Zhang, D. H.; Zhou, Q. F.; Shung, K. K.; Zhou, C. Nanowire Transistors with Ferroelectric Gate Dielectrics: Enhanced Performance and Memory Effects. *Appl. Phys. Lett.* **2004**, *84*, 4553–4555.
29. Li, C.; Fan, W.; Straus, D. A.; Lei, B.; Asano, S.; Zhang, D.; Han, J.; Meyyappan, M.; Zhou, C. Charge Storage Behavior of Nanowire Transistors Functionalized with Bis(terpyridine)-Fe(II) Molecules: Dependence on Molecular Structure. *J. Am. Chem. Soc.* **2004**, *126*, 7750–7751.
30. Steinitz, M. Quantitation of the Blocking Effect of Tween 20 and Bovine Serum Albumin in ELISA Microwells. *Anal. Biochem.* **2000**, *282*, 232–238.
31. Suwansa-ard, S. K. P.; Asawatreratanakul, P.; Wongkittisuksa, B.; Limsakul, C.; Thavarungkul, P. Comparison of Surface Plasmon Resonance and Capacitive Immunosensors for Cancer Antigen 125 Detection in Human Serum Samples. *Biosens. Bioelectron.* **2009**, *24*, 3436–3441.
32. Langmuir, I. The Constitution and Fundamental Properties of Solids and Liquids Part I Solids. *J. Am. Chem. Soc.* **1916**, *38*, 2221–2295.
33. Halperin, A.; Buhot, A.; Zhulina, E. B. On the Hybridization Isotherms of DNA Microarrays: the Langmuir Model and its Extensions. *J. Phys.: Condens. Matter* **2006**, *18*, S463–S490.
34. Ishikawa, F. C.; Chang, H.-K.; Curreli, M.; Chen, P.; Zhang, R.; Roberts, R.; Sun, R.; Cote, R.; Thompson, M.; Zhou, C. Label-Free, Electrical Detection of the SARS Virus N-Protein with Nanowire Biosensors Utilizing Antibody Mimics as Capture Probes. *ACS Nano* **2009**, *3*, 1219–1224.